

New Method to Estimate Binary Mass Ratios by Using Superhumps

Taichi KATO

Department of Astronomy, Kyoto University, Sakyo-ku, Kyoto 606-8502
tkato@kusastro.kyoto-u.ac.jp

and

Yoji OSAKI

Department of Astronomy, School of Science, University of Tokyo, Hongo, Tokyo 113-0033
osaki@ruby.ocn.ne.jp

(Received 201 0; accepted 201 0)

Abstract

We propose a new dynamical method to estimate binary mass ratios by using the period of superhumps in SU UMa-type dwarf novae during the growing stage (the stage A superhumps). This method is based on a working hypothesis in which the period of the superhumps at the growing stage is determined by the dynamical precession rate at the 3:1 resonance radius, a picture suggested in our new interpretation of the superhump period evolution during the superoutburst (Osaki, Kato 2013). By comparison with the objects with known mass ratios, we show that our method can provide sufficiently accurate mass ratios comparable to those obtained by quiescent eclipse observations. This method is very advantageous in that it requires neither eclipses, nor an experimental calibration. It is particularly suited for exploring the low mass-ratio end of the evolution of cataclysmic variables, where the secondary is undetectable by conventional methods. Our analysis suggests that previous estimates of mass ratios using superhump periods during superoutburst were systematically underestimated for low mass-ratio systems and we provided a new calibration. It suggests that most of WZ Sge-type dwarf novae have secondaries close to the border of the lower main-sequence and brown dwarfs, and most of the objects have not yet reached the evolutionary stage of period bouncers. Our result is not in contradiction with an assumption that the observed minimum period (~ 77 min) of ordinary hydrogen-rich cataclysmic variables is indeed the period minimum. We highlight the importance of early observation of stage A superhumps and propose a future desirable strategy of observation.

Key words: accretion, accretion disks — stars: dwarf novae — stars: novae, cataclysmic variables

1. Introduction

Cataclysmic variables (CVs) are close binary systems composed of a white dwarf primary and a red-dwarf or brown-dwarf secondary transferring matter via Roche overflow [for a review of CVs, see Warner (1995); Hellier (2001)]. The transferred matter forms an accretion disk around the white dwarf. Dwarf novae (DNe) are a class of CVs that undergo recurrent outbursts, whose origin is believed to be the thermal instability in the accretion disk. SU UMa-type dwarf novae are a subclass of DNe that show long-lasting outbursts called superoutbursts and superhumps during superoutbursts. The origin of superhumps is generally believed to be the tidal instability (Whitehurst 1988) generated at the radius in 3:1 resonance with the orbital motion of the secondary. In the thermal-tidal instability (TTI) model (Osaki 1989), the superoutburst is triggered by an outburst which produces an expansion of the accretion disk to the radius of the 3:1 resonance and thereby excites the tidal instability to produces superhumps¹ and strong tidal removal of the angular momentum from the disk [for a review, see Osaki (1996)].

There is a long history to try to extract the elusive mass ratio $q = M_2/M_1$ of the binary from the fractional superhump (SH) excess in period, which is defined by $\varepsilon \equiv P_{\text{SH}}/P_{\text{orb}} - 1$ where P_{SH} and P_{orb} are the superhump period and the orbital period of the binary, respectively. That is to try to estimate the binary's mass ratio q from easily observable superhump-period excess ε . It is convenient to introduce another expression, ε^* , the apsidal precession rate of the eccentric disk, ω_{pr} , over the binary orbital angular frequency, ω_{orb} , which is written as $\varepsilon^* \equiv \omega_{\text{pr}}/\omega_{\text{orb}} = 1 - P_{\text{orb}}/P_{\text{SH}}$. These two ε 's are related with each other by $\varepsilon^* = \varepsilon/(1 + \varepsilon)$ or $\varepsilon = \varepsilon^*/(1 - \varepsilon^*)$.

the superhump light source based on the enhanced mass transfer (EMT) model, in which the superhump may be produced by variable hot-spot brightness due to variable mass transfer rate which is in turn produced by periodic variation in irradiation heating of the secondary star. Our discussion presented in this paper can not be applied to Smak's EMT model. This is firstly because the basic underlying "clock" for variable irradiation in his model is rather vague as Smak (2009) has just mentioned it as "a tidal origin" and secondly because his model involves the time delay between enhanced irradiation heating on the surface of the secondary and enhanced mass transfer, Δt_{flow} , and this time delay is very uncertain because of uncertain nature of the hydrodynamic flow on the surface of the secondary.

¹ Smak (2009) has proposed an alternative model to the standard model of the tidal dissipation of the eccentric precessing disk for

The apsidal precession rate of an eccentric disk in SU UMa stars was first discussed by Osaki (1985), who showed that the precession rate is a function of the binary’s mass ratio, q , and the disk radius R_d because the apsidal precession rate of an accretion disk is basically determined by the gravitational tidal torques of the secondary star acting on the eccentric disk. Thus it was natural to use ε^* or ε for estimating q . This method was thus used to estimate the mass ratio for X-ray binaries (Mineshige et al. 1992), and for cataclysmic variable stars (Patterson 1998; Patterson et al. 2005 and refinements by various authors).

However, there are two problems in this approach. One is that the superhump period varies with time during a superoutburst and thus a question naturally arise at what stage we should apply the $\varepsilon - q$ relation. The other problem is that the the pressure effects within the disk contribute in determining the apsidal precession rate of the eccentric disk besides the pure dynamical effects of the secondary tidal torques and thus it is not a pure dynamical problem.

As for the first problem, through an extensive survey of SU UMa-type dwarf novae, Kato et al. (2009) have shown that the superhump periods in many SU UMa-type dwarf novae exhibit a characteristic pattern of variation where their $O - C$ diagrams show a variation with the stage A–B–C: (1) stage A with growing superhumps; the superhump period is longer than in other stages, (2) stage B with a shorter superhump period; in objects with short P_{orb} , the period derivative $P_{\text{dot}} \equiv \dot{P}/P$ is positive, i.e. the superhump period increases during this stage, (3) stage C with a shorter superhump period than in stage B; during stage C, the period is relatively constant and this stage often continues after the termination of the superoutburst (figure 1).

Kato et al. (2009) experimentally assumed that the period of the superhumps (or the fractional superhump excess) at the beginning of stage B reflects the precession rate at the 3:1 resonance. This selection was based on the finding that this period is very close to the superhump stable period of stage C in objects with $P_{\text{dot}} > 0$. Kato et al. (2009) regarded stage A superhumps as immature superhumps, and the fully mature superhump at the beginning of stage B reflects the fully grown 3:1 resonance. Using this assumption and using the dependence of the dynamical precession rate on the radius, Kato et al. (2009) estimated the disk radius variation in a purely dynamical way. This treatment, however, neglected the pressure effect.

As for the second problem of the pressure effects, it is known that they act to reduce the apsidal precession rate of the eccentric disk (Lubow 1992; Hirose, Osaki 1993; Murray 1998; Montgomery 2001; Pearson 2006). Among them Pearson (2006) showed that the pressure effect is necessary to express the observation, and derived the strength of the pressure effect for the calibration objects in Patterson et al. (2005) using the formulation by Lubow (1992).

In this paper, we propose a new dynamical method to

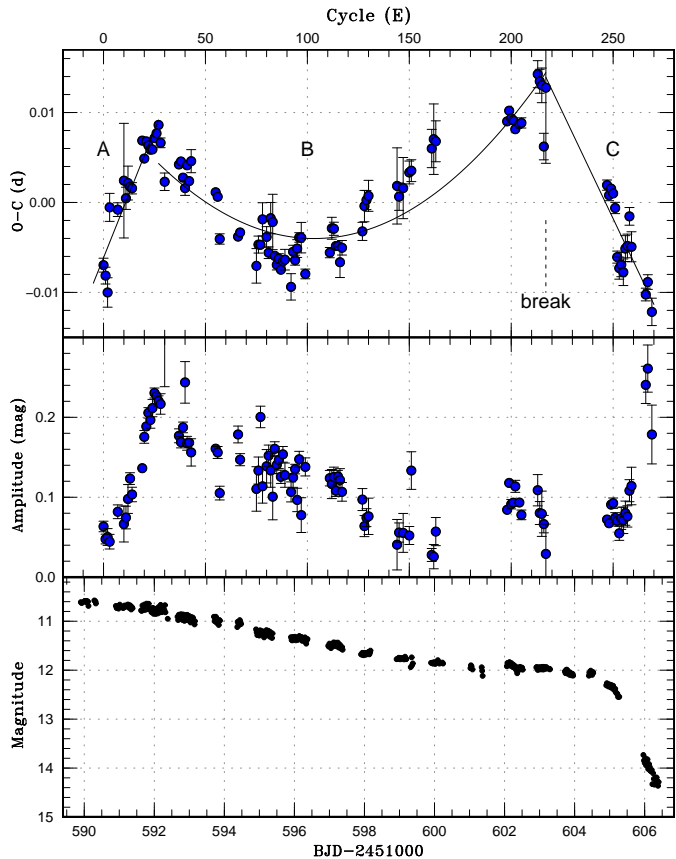


Fig. 1. Representative $O - C$ diagram showing three stages (A–C) of $O - C$ variation. The data were taken from the 2000 superoutburst of SW UMa. (Upper:) $O - C$ diagram. Three distinct stages (A – evolutionary stage with a longer superhump period, B – middle stage, and C – stage after transition to a shorter period) and the location of the period break between stages B and C are shown. (Middle:) Amplitude of superhumps. During stage A, the amplitude of the superhumps grew. (Lower:) Light curve.

estimate binary mass ratios by using the period of superhumps in SU UMa-type dwarf novae during the growing stage (the stage A superhumps), and examine the periods of superhumps recorded in Kato et al. (2009), Kato et al. (2010), Kato et al. (2012a), Kato et al. (2013). In section 2, we present the major premise of our working model and its formulation. In section 3 we present a test for the interpretation using a comparison with systems with known q and a comparison of the resultant evolutionary sequence. In section 4 we present various applications and implications.

2. The Main Premise of Our Working Model and Its Formulation

Osaki, Kato (2013) have proposed a new interpretation for the time evolution of the superhump period during superoutbursts of V344 Lyr and V1504 Cyg in the Kepler data, in particular by using a comparison of simultaneously recorded positive and negative superhumps. In SU

UMA stars, the longest superhump period (and therefore the highest apsidal precession rate) occurs at the growing stage of the superhump (stage A in Kato et al. 2009 classification). Osaki, Kato (2013) have interpreted that this is most likely given by that corresponding to the dynamical precession rate at the 3:1 resonance radius. Its following rapid decrease in the SH period (a transition from stage A to stage B) is then understood as due to propagation of the eccentricity wave to the inner part of the disk by which a larger portion of the disk is involved in determining the precession rate of the whole disk.

In this interpretation, the dynamical precession rate at the 3:1 resonance is represented in the growing stage of superhumps (stage A) when the eccentric wave is still confined to the location of the resonance. In this paper we adopt this interpretation as our working model and we examine its consequence below. This interpretation leads to an important consequence: q can be directly determined (without an experimental coefficient) by a dynamical way from ε^* of the stage A superhumps. The traditional way of using ε^* for stage B superhumps to estimate q (e.g. Patterson et al. 2005; Kato et al. 2009) suffers from the unknown pressure effect, which is expected to be the strongest in stage B, resulting large uncertainties.

The dynamical precession rate, ω_{dyn} , at radius r in the disk can be expressed by (see, Hirose, Osaki 1990)

$$\begin{aligned} \omega_{\text{dyn}}/\omega_{\text{orb}} &= \frac{q}{\sqrt{1+q}} \left[\frac{1}{4} \frac{1}{\sqrt{r}} \frac{d}{dr} \left(r^2 \frac{db_{1/2}^{(0)}}{dr} \right) \right] \\ &= \frac{q}{\sqrt{1+q}} \left[\frac{1}{4} \frac{1}{\sqrt{r}} b_{3/2}^{(1)} \right], \end{aligned} \quad (1)$$

where r is the dimensionless radius measured in units of the binary separation A , ω_{orb} is the angular frequency of the binary motion, and $\frac{1}{2}b_{s/2}^{(j)}$ is the Laplace coefficient

$$\frac{1}{2}b_{s/2}^{(j)}(r) = \frac{1}{2\pi} \int_0^{2\pi} \frac{\cos(j\phi)d\phi}{(1+r^2-2r\cos\phi)^{s/2}}, \quad (2)$$

We estimate the dynamical precession rate at the 3:1 resonance radius, which is given by

$$r_{3:1} = 3^{(-2/3)}(1+q)^{-1/3}. \quad (3)$$

We can now calculate the dynamical precession rate of the eccentric disk at the 3:1 resonance radius and we show our results in table 1 and figure 2 for $\varepsilon^* - q$ relation. We also give approximate analytic formulae as follows:

$$\varepsilon^* = 0.00027 + 0.402q - 0.467q^2 + 0.297q^3, \quad (4)$$

which has a maximum error 0.00004 in ε^* and

$$q = -0.0016 + 2.60\varepsilon^* + 3.33(\varepsilon^*)^2 + 79.0(\varepsilon^*)^3, \quad (5)$$

which has a maximum error 0.0004 in q , respectively, in the range of $0.025 \leq q \leq 0.394$. Since numerical integration using equation (2) converges sufficiently quickly, we recommend to use integration rather than polynomial approximations.

By identifying the observed ε^* for stage A superhumps to the dynamical precession rate at the 3:1 resonance radius, we can obtain q . This is our basic strategy in this

Table 1. Relation between ε^* of stage A and q .

ε^*	q	ε^*	q	ε^*	q
0.010	0.025	0.042	0.119	0.074	0.241
0.012	0.030	0.044	0.126	0.076	0.250
0.014	0.036	0.046	0.133	0.078	0.259
0.016	0.041	0.048	0.140	0.080	0.268
0.018	0.047	0.050	0.147	0.082	0.277
0.020	0.052	0.052	0.154	0.084	0.287
0.022	0.058	0.054	0.161	0.086	0.296
0.024	0.064	0.056	0.168	0.088	0.306
0.026	0.069	0.058	0.176	0.090	0.317
0.028	0.075	0.060	0.183	0.092	0.327
0.030	0.081	0.062	0.191	0.094	0.337
0.032	0.087	0.064	0.199	0.096	0.348
0.034	0.093	0.066	0.207	0.098	0.359
0.036	0.100	0.068	0.215	0.100	0.370
0.038	0.106	0.070	0.224	0.102	0.382
0.040	0.113	0.072	0.232	0.104	0.394

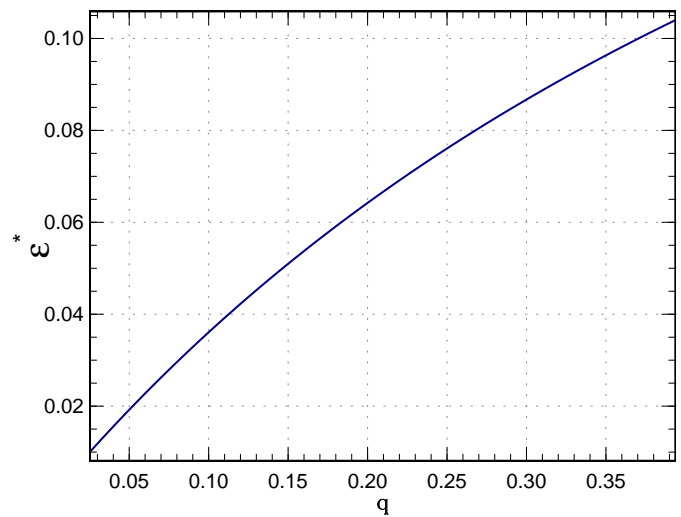


Fig. 2. Relation between ε^* of stage A and q .

paper.

We now compare our interpretation with the smoothed particle hydrodynamics (SPH) simulations of superhumps by Murray (1998), who demonstrated the evolution of the superhump period for one of his simulations in a form of $O-C$ diagram. His $O-C$ diagram showed a pattern similar to stage A–B transition during the growing stage of superhumps. Our result is now compared with SPH result [Murray (1998), $P_{\text{SH}}/P_{\text{orb}}$ (max) corresponding to stage A]. The agreement is fair: $\varepsilon^*=0.090$ for $q=0.25$, $\varepsilon^*=0.065-0.069$ for $q=3/17=0.176$ and $\varepsilon^*=0.049$ for $q=1/9=0.111$. Considering the intrinsic difficulty in measuring the periods from SPH simulations, the agreement appears to be sufficient.

Since the SPH simulations are favorably compared with our interpretation, let us turn to observations.

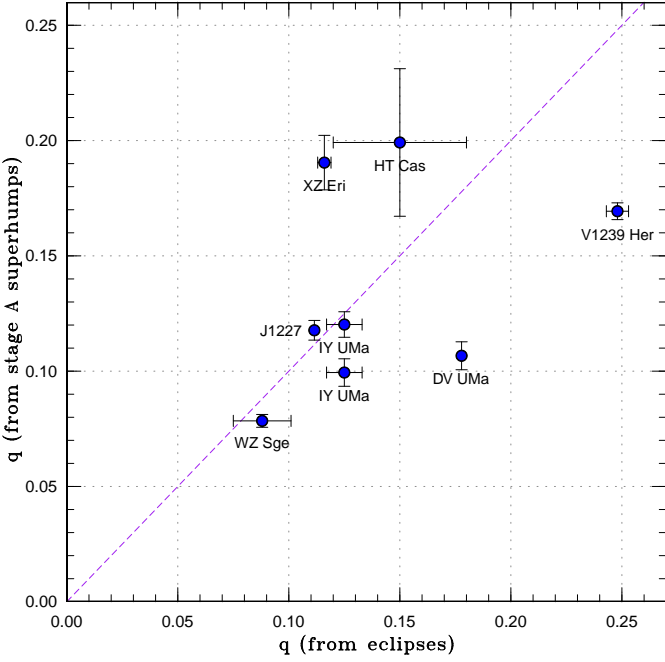


Fig. 3. Comparison of q measured from eclipse (abscissa) and q estimated from stage A superhump based on our method (ordinate). The names of the objects are given with labels (J1227 stands for SDSS J122740.83+513925.0) IY UMa has two observations (2000 and 2009), which are plotted individually. The values of measured q for all objects other than WZ Sge were derived from eclipse observations, while estimated q are those obtained from superhump periods at the stage A by our method.

3. Comparison with Observations

3.1. Stage A Superhumps in Systems with Known Mass Ratios

Some objects have known mass ratios determined from quiescent eclipse observations. These objects are listed in table 2 together with WZ Sge, which has constraint on q from Doppler tomography (Steeghs et al. 2001). We have determined the q from stage A superhumps by our method described in section 2, and made a comparison with the observed q .

As the first step, we made a comparison of the estimated q from all known stage A superhumps by our method and q from quiescent eclipse observations to see what quality of observation is needed to make this estimate. The result is shown in figure 3. Since there are intrinsic difficulties both in eclipse observations and observation of stage A superhumps, there remain a relatively large scatter in some objects. The agreement is, however, good for objects with both reliable eclipse observations and well-covered stage A observation.

The problem for each object can be summarized as follows.

V1239 Her: There were only three superhump measurements in stage A, and the period was determined assuming that stage A continued to $E = 22$ (Kato et al. 2013). If

stage A–B transition took place earlier, the period of stage A should be longer. The present analysis would favor this interpretation. This period appears to be inadequate for a comparison.

DV UMa: The eclipses of this object are deep, and it was difficult to determine the times of stage A superhumps. The combined $O-C$ diagram showed a large scatter (Kato et al. 2012a). Although the 2007 data were used to make the present comparison, possible stage A superhumps were also detected in the 1997 data (Patterson et al. 2000; Kato et al. 2009). Using $E \leq 12$ maxima for the 1997 data, we obtained a period of 0.0933(9) d. This period gave $q=0.26$, which appears too large. The period of stage A superhumps in this object needs to be re-examined by future observations.

HT Cas: The measurement by Horne et al. (1991) was rather old, and the weakness of the hot spot in this object would make the eclipse analysis difficult [e.g. Feline et al. (2005)]. Ioannou et al. (1999) favored a different q value. It appears that q value is still uncertain for this object. Despite the very good coverage of the 2010 superoutburst (Kato et al. 2012a), the eclipses unfortunately overlapped the superhump maxima around this phase (see figure 9 in Kato et al. 2012a) and the period of stage A superhumps was very inaccurate. This period appears to be inadequate for a comparison.

XZ Eri: The 2008 data were used. There were only five measurements of superhump maxima with relatively large errors (Kato et al. 2009). A combined $O-C$ diagram with the 2007 observation (figure 87 in Kato et al. 2009) appears to suggest a shorter period for stage A superhumps. The period of stage A superhumps in this object again needs to be re-examined by future observations.

Considering these uncertainties and difficulties, direct comparisons of q values from eclipse observations and stage A superhumps will continue to be the challenges of the future. We can, however, safely say there does not appear to be a strongly contradicting case at least for low- q objects.

3.2. Evaluation of q from Stage A Superhump and $P_{\text{orb}} - q$ Relation

Although a comparison between q values from stage A superhumps and from quiescent eclipse observation is most direct, it suffers from the small number of objects and lower quality of stage A observation due to eclipses. We therefore took an alternative approach in which we examine the relation between the binary orbital period P_{orb} and the mass ratio q estimated from stage A superhumps by our method for a much larger sample of both eclipsing and non-eclipsing SU UMa stars.

From evolutionary consideration of the cataclysmic variable stars, it is well known (e.g. Knigge 2006) that there is a definite relation between the orbital period, P_{orb} , and the mass of the secondary star ($P_{\text{orb}} - M_2$ relation) and if we assume some certain mass for the primary white dwarf [M_1 ; Savoury et al. (2011) showed that the mean $M_1=0.83 M_{\odot}$ with an intrinsic scatter of $0.07 M_{\odot}$ for systems with $P_{\text{orb}} \leq 0.066$ d.], we can translate it to $P_{\text{orb}} - q$

q systems and the eccentric region spreads more quickly than in low- q systems. This lesson would tell us we should pay more attention to choosing a segment of observations when analyzing objects with long- P_{orb} or higher- q objects. The value of 0.07395(21) d in Kato et al. (2012a) corresponds to $q=0.181(10)$. The revised value is within 1σ of the value derived from the entire stage A superhumps in an ordinary superoutburst, and these measurements are not in serious contradiction.

The result is shown in figure 4 for the $P_{\text{orb}} - q$ relation. In table 3, we also listed q values in Patterson (2011) (P11). Most of his q values were determined from ε for stage B superhumps using the empirical relation in Patterson et al. (2005). For objects with high-quality stage A measurements, the agreement between these two methods is very good for q larger than 0.085–0.090, indicating that our method is consistent with the previous method at least for higher- q objects. Patterson et al. (2005) used an older P_{orb} for V342 Cam [0.0763 d, one of the candidate aliases listed in Aungwerojwit et al. (2006), see Kato et al. (2009) for the selection], and the difference between the estimated q values was caused by this period selection. If we use the older value, we obtain $q=0.121(4)$, perfectly in agreement.

The agreement is, however, worse for lower q objects. This is particularly clearly seen in WZ Sge, for which Patterson (2011) gave $q=0.046$ in contrast to our $q=0.078(3)$. Patterson (2011) seems to have underestimated q for low- q objects, i.e. WZ Sge-type dwarf novae. This can be understood as follows: Patterson (2011) used stage B superhumps, which is strongly affected by the pressure effect and the relative strength of the pressure effect depends on q , i.e. lower q objects has a stronger pressure effect (Kato, Osaki 2013; later discussion in this paper). Since Patterson (2011) used a nearly linear $\varepsilon - q$ relation for low- q and assumed $\varepsilon = 0$ for $q = 0$, this pressure effect was translated to a systematically smaller q . This systematic trend would affect the discussion for the evolution of low- q objects, i.e. the objects near or after the period minimum. For example, systematically smaller q will increase the fraction of brown-dwarf secondaries or period bouncers. Our figure 4 suggests that most of the dwarf novae have not yet reached the period minimum.

One notable object is OT J184228. This object was suggested to be a period bouncer using the ε for stage B superhumps (which were only seen during its second outburst; Kato et al. 2013). The present conclusion from stage A superhumps well agrees with the previous identification.

3.2.2. Comparison of q Values with Those from Quiescent Eclipse Observation

In recent years, the advent of high-speed CCD photometry and the use of Markov-chain Monte Carlo (MCMC) modeling of the light curve have made great improvement in measuring binary parameters (Littlefair et al. 2008; Southworth, Copperwheat 2011) than in the 1990s. We can now use more reliable set of q measurements than in the time of Patterson et al. (2005), Knigge (2006).

A comparison of q estimated from stage A super-

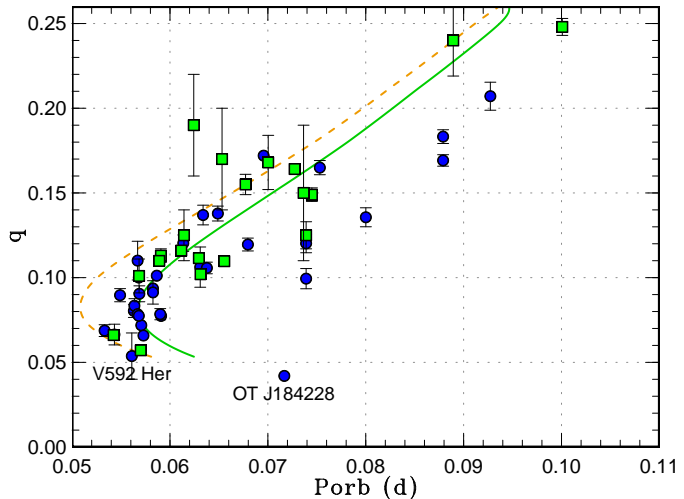


Fig. 5. Comparison of q estimated by our method from stage A superhumps (filled circles) and q measured by eclipses (filled squares). The agreement is very good. The dashed and solid curves represent the standard and optimal evolutionary tracks in Knigge et al. (2011), respectively. Our new q values support the discussion on the evolutionary sequence in Littlefair et al. (2008) and Knigge et al. (2011) in that an angular momentum loss larger than solely from the gravitational wave radiation is needed to reproduce the $P_{\text{orb}}-q$ relation.

humps and q measured by eclipses is given in figure 5. In addition to the objects in table 2, we included Z Cha (Wade, Horne 1988), OY Car (Littlefair et al. 2008), 1RXS J180834.7+101041, V1258 Cen, CTCV J2354–4700, SDSS J115207.00+404947.8, OU Vir, SDSS J103533.02+055158.3, SDSS J090350.73+330036.1, SDSS J143317.78+101123.3, NZ Boo, SDSS J150137.22+550123.4 (Southworth, Copperwheat 2011), V2051 Oph (Baptista et al. 1998), SDSS J152419.33+220920.0 (Southworth et al. 2010) and V4140 Sgr (Borges, Baptista 2005). The agreement of the evolutionary sequence between two types of measurements is very good. The outlier in the upper left corner is V2051 Oph, whose quality of parameter estimation may have not been so good. This figure corresponds to figure 6 in Littlefair et al. (2008) with a much higher number of q estimates.

We have seen both in direct comparison and in comparison of the inferred evolutionary sequence that q values from stage A superhumps are reliable and as accurate as those from determined from quiescent eclipse observations. We can therefore adopt the assumption that stage A superhumps indeed reflect the dynamical precession rate at the radius of the 3:1 resonance. We should note, however, the result by our method appears to give smaller q for long- P_{orb} objects. We suspect that this is caused by insufficient observational coverage for early part of stage A superhumps in these objects, since these objects took shorter time to develop superhumps, and the early stage A evolution tends to be missed by observation. This difficulty is apparently avoided for short- P_{orb} objects because

Table 3. q estimated from stage A superhumps by our method.

Object	Year	$P_{\text{orb}}^{*\dagger}$	P_{SH}^* (stage A)	q (by our method)	q (from P11) \ddagger	Quality §	References $^{\parallel}$
Kato et al. (2009)							
V455 And	2007	0.05631	0.05803(8)	0.080(4)	0.06	1	1, 2
V466 And	2008	0.05636	0.05815(8)	0.083(4)	0.058	1	2, 2
VY Aqr	2008	0.06309(4)	0.06558(26)	0.106(12)	0.095	1	3, 2
V342 Cam	2008	0.07531(8)	0.07970(10)	0.164(4)	0.121	1	4, 2
WX Cet	1989	0.05826	0.06031(3)	0.094(1)	0.094	1	5, 2
	1998		0.06027(14)	0.091(7)		1	2
HO Cet	2006	0.05490(2)	0.05676(7)	0.090(4)	0.091	1	2, 2
PU CMa	2008	0.05669(4)	0.05901(22)	0.110(11)	0.109	2	6, 2
V632 Cyg	2008	0.06377(8)	0.06628(7)	0.106(3)	0.125	2	7, 2
GW Lib	2007	0.05332(2)	0.05473(7)	0.069(3)	0.056	1	8, 2
V453 Nor	2005	0.06338(4)	0.06653(12)	0.137(6)	0.082	1	9, 2
UV Per	2003	0.06489(1)	0.06813(9)	0.138(4)	0.108	1	3, 2
V493 Ser	2007	0.08001(1)	0.08395(14)	0.136(6)	0.156	2	10, 2
WZ Sge	2001	0.05669	0.05838(6)	0.078(3)	0.046	1	11, 2
SW UMa	2006	0.05681	0.05894(5)	0.100(3)	0.113	1	12, 2
IY UMa	2000	0.07391	0.07666(15)	0.099(6)	0.12	1	13, 2
KS UMa	2003	0.06796(10)	0.07095(8)	0.120(4)	0.112	1	14, 2
HV Vir	2002	0.05707	0.05864(2)	0.072(1)	0.094	2	14, 2
ASAS J1025	2006	0.06136(6)	0.06407(10)	0.120(5)	0.135	1	2, 2
Kato et al. (2010)							
V592 Her	2010	0.05610 [#]	0.05728(29)	0.054(14)	0.037?	2	15, 15
IY UMa	2009	0.07391	0.07717(14)	0.120(6)	0.12	1	12, 15
SDSS J1610	2009	0.05687(1)	0.05881(9)	0.090(5)	0.086	1	15, 15
OT J1044	2010	0.05909(1)	0.06084(3)	0.077(1)	–	2	15, 15
Kato et al. (2012a)							
EZ Lyn	2010	0.05901	0.06077(7)	0.078(3)	0.05	1	16, 16
V344 Lyr	2009	0.08790	0.09314(9)	0.169(3)	–	1	17, 16
V344 Lyr	2009b	0.08790	0.09351(10)	0.183(4)	–	1	17, 16
SW UMa	2010	0.05681	0.05850(2)	0.077(1)	0.113	2	11, 16
V355 UMa	2011	0.05729	0.05874(3)	0.066(1)	–	1	18, 16
Kato et al. (2013)							
BW Scl	2011	0.05432	0.05572(12)	0.067(6)	–	1	19, 20
OT J184228	2011	0.07168(1)	0.07287(8)	0.042(3)	–	1	20, 20
OT J210950	2011	0.05865 [#]	0.06087(6)	0.101(3)	–	2	20, 20
OT J214738	2011	0.09273 [#]	0.09928(22)	0.207(8)	–	1	20, 20
This paper							
V1504 Cyg	2009b	0.06955	0.07377(6)	0.172(2)	0.150	1	16, 21

*Unit d.

[†]The error is smaller than 1 in the last significant digit if the error is omitted.[‡] q value in Patterson (2011). Most of the values were determined from ε for stage B superhumps.[§]Quality of stage A observation. 1: good, 2: low quality.^{||}The two numbers refer to the references to P_{orb} and P_{SH} (stage A). 1: Araujo-Betancor et al. (2005); 2: Kato et al. (2009); 3: Thorstensen, Taylor (1997); 4: Shears et al. (2011); 5: Sterken et al. (2007); 6: Thorstensen, Fenton (2003); 7: Sheets et al. (2007); 8: Thorstensen et al. (2002); 9: Imada, Monard (2006); 10: Woudt et al. (2004), alias selection in Kato et al. (2009); 11: Patterson et al. (2002), Kato et al. (2009); 12: J. Thorstensen, PhD thesis 13: Steeghs et al. (2003); 14: Patterson et al. (2003); 15: Kato et al. (2010); 16: Kato et al. (2012a); 17: Osaki, Kato (2013); 18: Gänsicke et al. (2006), updated in Kato et al. (2012a); 19: Augusteyjn, Wisotzki (1997); 20: Kato et al. (2013). 21: this paper.[#]Tentative identification.

Abbreviations for the names: ASAS J102522–1542.4 (ASAS J1025), SDSS J161027.61+090738.4 (SDSS J1610), OT J104411.4+211307 = CSS100217:104411+211307 (OT J1044), OT J184228.1+483742 (OT J184228), OT J210950.5+134840 (OT J210950), OT J214738.4+244553 = CSS111004:214738+24455 (OT J214738).

they have a long waiting time before superhumps appears. This interpretation need to be checked by future observations.

4. Discussion

4.1. New Calibration for $\varepsilon - q$ Relation

Although we consider that the use of stage A superhumps is the first choice for estimating q for objects with well-observed stage A superhumps, this condition is not always met by observation. In such cases, we may use stage B superhumps to estimate q , as have been done traditionally, under a simplified assumption of the constant pressure effect for each q . One should remember that the pressure effect may different between different objects, and the treatment here may not be always valid.

By using q estimated from stage A superhumps, we can re-calibrate the $\varepsilon - q$ relation for a much larger sample than in Patterson et al. (2005) or Kato et al. (2009), which were mainly based on q values estimated by using relatively rare eclipsing systems. As the first step, we re-calibrate the frequently used $\varepsilon - q$ relation in Patterson et al. (2005) (and its improvement in Kato et al. 2009). In order to make a fair comparison with Patterson et al. (2005), we used ε estimated from P_{SH} tabulated in his paper by Patterson (2011) since ε is dependent on the outburst phase, and Patterson et al. (2005) apparently “estimated period 4 d after maximum light (or hump onset)” when this is available [footnote 11 of Patterson (2011)]. Since P_{SH} for WZ Sge was missing, we supplied it from Patterson et al. (2002). The result is shown in figure 6. The systematic departure from the relation in Patterson et al. (2005) is evident: q is always estimated lower for $\varepsilon \leq 0.018$. A linear fit yielded a new relation

$$q = 0.035(10) + 3.09(40)\varepsilon, \quad (6)$$

which may be used for superhump periods in the early phase (but not so early as stage A superhumps). This equation suggests that ε could be negative for $q \leq 0.035$ (i.e., retrograde precession for a sufficiently low q), and this is probably due to the stronger pressure effect in relation to the tidal effect in low- q systems.

Although this functional form is not theoretically derived, we may have a qualitative interpretation. According to Lubow (1992), the apsidal precession rate (ν_{pr}) can be written as a form:

$$\nu_{\text{pr}} = \nu_{\text{dyn}} + \nu_{\text{pressure}} + \nu_{\text{stress}}, \quad (7)$$

where the first term, ν_{dyn} , represents a contribution to disk precession due to tidal perturbing force of the secondary, giving rise to prograde precession, the second term, ν_{pressure} , the pressure effect giving rise to retrograde precession, and the last term, ν_{stress} , the minor wave-wave interaction. While ν_{dyn} is dependent on q (roughly $\propto q$), ν_{pressure} is independent of q , suggesting a functional form like $\varepsilon \sim a \times q - \text{const.}$, a linear relation between ε and q . Although this effect was also noticed in the analyses by Pearson (2006) and Goodchild, Ogilvie (2006), their samples were a mixed class of objects from Patterson et al.

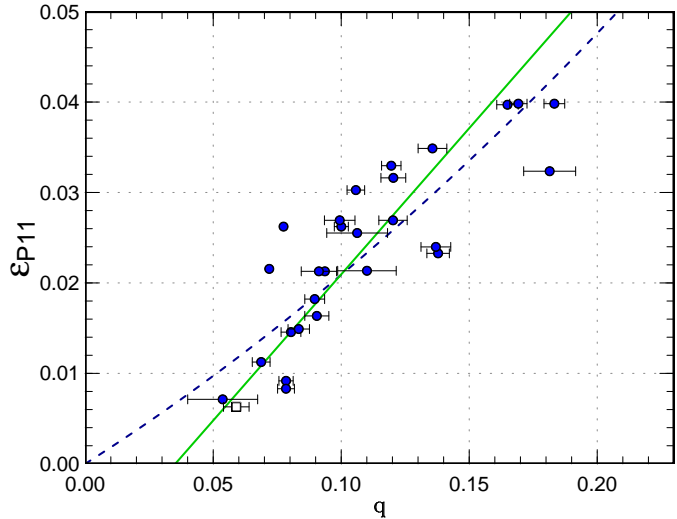


Fig. 6. Relation between ε (Patterson 2011) and q estimated from stage A superhumps. The dashed curve and solid line represent the relation in Patterson et al. (2005) and a linear fit, respectively. The open rectangle represents EG Cnc, estimated from post-superoutburst superhumps (see subsection 4.3.1), which was not used for the regression.

(2005). The actual treatment of the precession rate in the presence of pressure, however, is more complex in terms of eigenfunction expression (cf. Hirose, Osaki 1993; Osaki, Kato 2013).

Similarly, we obtained a relation for the middle (mean) of stage B superhumps (values from Kato et al. 2009, Kato et al. 2010, Kato et al. 2012a, Kato et al. 2013) as follows:

$$q = 0.026(7) + 3.36(27)\varepsilon. \quad (8)$$

Although these regressions appear useful within the limit of observational scatter, a linear regression on the $q - \varepsilon$ space cannot properly take into account of the non-linear dependence of ε on q (we therefore do not recommend to use figures 6, 7 to estimate q). We instead may better use the value of ε^* at the 3:1 resonance radius (i.e., the value of ε^* for stage A superhumps) to represent q and we find a relation between observed ε and this dynamical precession rate ε^* in representing q . This method is expected to better deal with the non-linear functional form of ε^* against q . Once this relation is obtained, one can estimate the dynamical precession rate for the 3:1 resonance radius from the observed ε , and then convert the dynamical precession rate into q using the relation in section 2 (such as table 1 or figure 2). The result is shown in figure 8. The presence of a curvature of the relation by Patterson et al. (2005) on this plot now clearly demonstrates the cause of the systematic errors for low- q objects using the relation in Patterson et al. (2005). The linear regression is

$$\varepsilon^*(3:1) = 0.016(3) + 0.94(12)\varepsilon. \quad (9)$$

We recommend to use this relation rather than equations (6) and (8) to estimate q from early stage (early stage B)

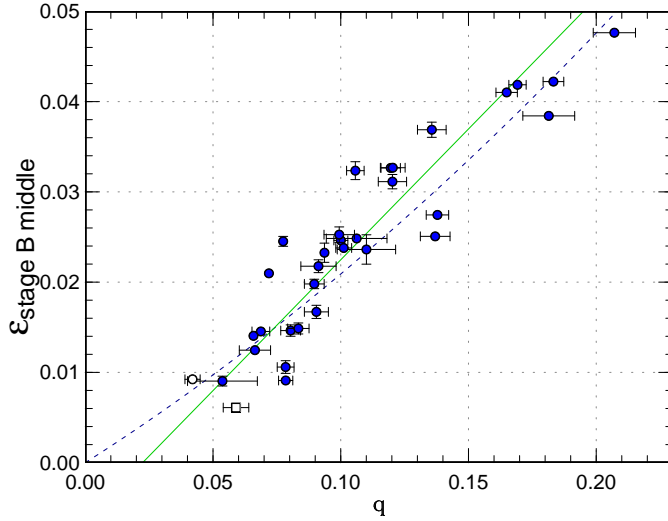


Fig. 7. Relation between ε for the middle (mean) of stage B superhumps and q estimated from stage A superhumps. The dashed curve and solid line represent the relation in Patterson et al. (2005) and a linear fit, respectively. The open circle represents the unusual object OT J184228. The open rectangle represents EG Cnc, estimated from post-superoutburst superhumps (see section 4.3.1). Both objects were not used for the regression.

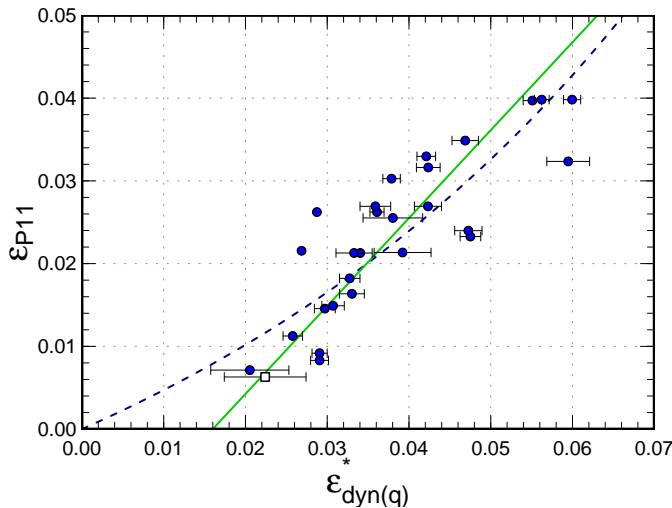


Fig. 8. Relation between ε (Patterson 2011) and ε^* stage A superhumps which represents q . The dashed curve and solid line represent the relation in Patterson et al. (2005) and a linear fit, respectively. The open rectangle represents EG Cnc, estimated from post-superoutburst superhumps (see subsection 4.3.1), which was not used for the regression.

superhump observations.

Figure 10 is the same relation for the middle (mean) of stage B superhumps. The relation is

$$\varepsilon^*(3:1) = 0.012(2) + 1.04(8)\varepsilon. \quad (10)$$

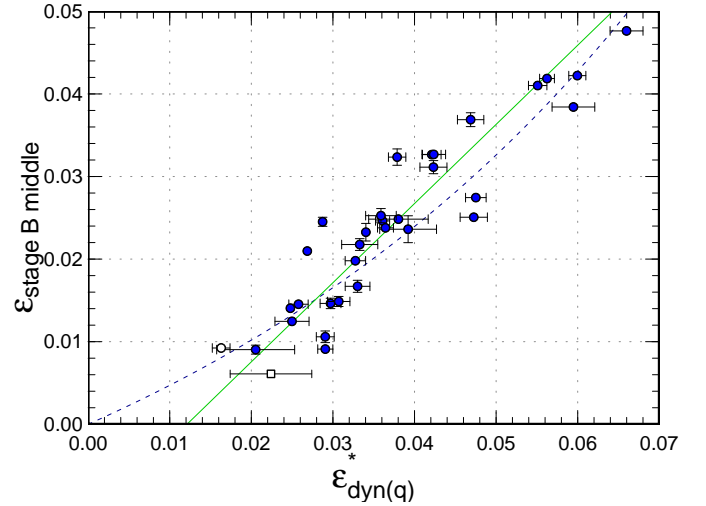


Fig. 9. Relation between ε for the middle (mean) of stage B superhumps and ε^* stage A superhumps which represents q . The dashed curve and solid line represent the relation in Patterson et al. (2005) and a linear fit, respectively. The open rectangle represents EG Cnc, estimated from post-superoutburst superhumps (see subsection 4.3.1), which was not used for the regression.

4.2. Implication to CV Evolution

The new q values estimated from stage A superhumps make the largest difference in low- q or short- P_{orb} systems, i.e. WZ Sge-type dwarf novae. Since the case of WZ Sge itself has been long discussed, here we examine this case. Despite a huge amount of efforts, the nature of the secondary in WZ Sge is still unclear. Steeghs et al. (2001) first succeeded in detecting the emission from the secondary in the Doppler tomography, and Steeghs et al. (2007) combined the ultraviolet radial velocity to estimate $M_1=0.85(4)M_\odot$ and $M_2=0.078(6)M_\odot$. Patterson et al. (2002), however, argued that q should be smaller considering the $M_K \sim 9.5$ for a $0.09M_\odot$ secondary which contradict with $M_K > 12.2$ derived from a trigonometric distance of $43(2)$ pc (Thorstensen 2003) and the absence of the secondary feature in the spectrum. Patterson (2011) preferred a very low mass secondary, $q = 0.045$.

Our result suggests $q=0.078(3)$, and using Steeghs et al. (2007), we obtained $M_2=0.066(4)M_\odot$. This mass corresponds to a brown dwarf having $M_K=10.6\text{--}11.1$ (Knigge 2006). Harrison et al. (2013) recorded the near-/mid-infrared variation attributable to ellipsoidal modulations of an L2-type secondary having $M_K=11.1$. Harrison et al. (2013) estimated that the secondary contributes to 80% at the eclipse minimum, and raised a question why the expected CO absorption for an L2 brown dwarf has not yet been detected. Our mass estimate higher than Patterson et al. (2002) supports the result by Harrison et al. (2013) and the secondary of WZ Sge is likely an object on the borderline of the end of the main sequence ($M_K \sim 11$) and brown dwarfs.²

² In reality, the popular Kumar limit ($\sim 0.075 M_\odot$) for core hy-

The q value for WZ Sge is slightly higher than the value of $q=0.0661(7)$ for SDSS J143317.78+101123.3, the eclipsing object with a system parameter ($P_{\text{orb}}=0.05424$ d) close to WZ Sge. The secondary of this object has recently been identified as an L2-type brown dwarf (Littlefair et al. 2013). There have been another detection of a brown dwarf in the eclipsing system SDSS 103533.03+055158.4 having $P_{\text{orb}}=0.057007$ d and $q=0.055(2)$ (Littlefair et al. 2006b). Since the latter two objects were more white dwarf-dominated in the spectrum and the eclipse light curves, these objects can be naturally understood as objects that passed the evolutionary stage of WZ Sge.

There has been a lot of discussions regarding the value of the period minimum and on the observational evidence for its presence. While the standard evolutionary model of CVs gives a shorter period (65–70 min, Kolb, Baraffe 1999; Howell et al. 2001), this value is much shorter than the minimum orbital period of ordinary hydrogen-rich CVs (Kolb 1993). Gänsicke et al. (2009) detected a high concentration of CVs near the period of ~ 80 min using the sample selected by the Sloan Digital Sky Survey (SDSS). Woudt et al. (2012) used the sample based on the Catalina Real-Time Survey (CRTS) and reached a similar conclusion. These authors used the distribution of P_{orb} for discussion. The P_{orb} distribution of dwarf novae detected as transients, however, can be biased due to the very low outburst frequency near the period minimum. Considering this bias, Uemura et al. (2010) applied a Bayesian approach to estimate the parent population, and obtained a shorter period minimum of ~ 70 min assuming a certain functional form for the P_{orb} distribution. Kato et al. (2012b) applied the same method to the neural network-based P_{orb} estimates using the SDSS colors of CRTS-selected objects. Although the latter method has a potential to estimate P_{orb} for a large number of less biased transients, it still suffers from the spread of the distribution due to estimation errors, and it allows a lower period minimum. Our present method can provide the q distribution against P_{orb} even for faint objects, and is more sensitive to the CV evolution than the distribution of P_{orb} alone. Our new result indicates that q starts to decrease quickly around $P_{\text{orb}} \simeq 80$ min, and the evolutionary sequence appears to approach the period minimum around this period. Our result is not in contradiction with an assumption that the observed minimum period (~ 77 min) is indeed the period minimum. This discussion, however, ignores the intrinsic spread of the period minimum and a more sophisticated treatment, as well as the increase of the sample including ones in the region of period bouncers, is required to make a more decisive discussion.

In subsection 3.2.2, we suggested that the result by our method appears to give smaller q for long- P_{orb} objects. This is more apparent when we compare the result with

drogen burning has no great significance in the case of CV evolution. The surface temperature of the secondary can depend on the age and evolution history. We use the term “brown dwarf” in the popular sense when describing the CV secondaries, and mean secondaries with masses somewhere below $0.05\text{--}0.09 M_{\odot}$ (Patterson 2011).

the theoretical evolutionary sequence (figures 4, 5). Since the Kepler data for V344 Lyr, which was not affected by the lack of early stage A observations, deviates from the theoretical evolutionary sequence, there may be a wider intrinsic spread of q in long- P_{orb} systems than in short- P_{orb} systems. This possibility needs to be tested by a larger sample.

4.3. Disk Radius in Post-superoutburst Stage

4.3.1. Disk Radius in WZ Sge-Type Dwarf Novae in Post-Superoutburst

Another good application to the present method would be to estimate the disk radius using superhumps long after the superoutburst. Since the disk is sufficiently cold in such a situation, we can expect that the superhump wave is confined to the disk’s outer edge, and we can ignore the pressure effect. Such persistent superhumps have been particularly well observed in WZ Sge-type dwarf novae. Kato et al. (2008) estimated the radius by assuming that stage B superhump represents the 3:1 resonance and concluded that these modulations are superhumps arising from matter near the tidal truncation radius. Since the new assumption is very different from the one at the time of Kato et al. (2008), we re-estimated the radius. The results are listed in table 4. It has become evident that there are two groups: objects with a large disk radius (0.37–0.38 A : GW Lib, V455 And, BW Scl) and ones with a small disk radius (0.30–0.32 A : WZ Sge, EZ Lyn). These groups correspond to WZ Sge-type dwarf novae without rebrightenings and with multiple rebrightenings, respectively. It would suggest that the remnant disk matter is larger if no rebrightenings occurs. While the smaller one appears to agree to what was supposed in Osaki (1995), the larger one is much larger than this.

If these radii for the WZ Sge-type dwarf novae in the post-superoutburst state is universal, we may estimate q by using the period of the post-superoutburst superhumps. A notable example is EG Cnc (Patterson et al. 1998), which showed a period of 0.06051(2) d (value refined in Kato et al. 2009). EG Cnc is a system with multiple rebrightenings (Patterson et al. 1998; Kato et al. 2004a), and we assume a disk radius of 0.31 A . The resultant $q=0.059(5)$, which is again larger than $q = 0.035$ in Patterson (2011). This value seems to be consistent with the updated empirical $\varepsilon - q$ (figure 6).

4.3.2. Disk Radius from Stage C Superhumps

The same procedure may be applied to stage C superhumps, though the disk is hotter than the fully post-superoutburst disk in WZ Sge-type dwarf novae and there may be remaining pressure effect. Since stage C superhumps often continue to exist after the termination of the superoutburst, we nevertheless estimated the disk radius by the same method used above. The results are shown in table 5 and figure 10. We note here that these results should be looked at with a caveat mentioned above. The majority of the objects have a disk radius $0.35 \pm 0.04A$, which is not very different from that estimated from post-superoutburst superhumps in WZ Sge-type dwarf novae. By using this assumption, we may estimate q for objects

Table 4. Disk radii estimated from the periods of late-stage superhumps of WZ Sge-type dwarf novae.

Object	P_{orb}^*	P_{ish}^\dagger	q	R_d^\ddagger	References
GW Lib	0.05332(2)	0.054156(1)	0.069	0.38	Kato et al. (2008)
V455 And	0.05630921(1)	0.057280(4)	0.080	0.37	Kato et al. (2008)
WZ Sge	0.0566878460(3)	0.057408(4)	0.078	0.32	Kato et al. (2008)
EZ Lyn	0.05900495(3)	0.05967(2)	0.078	0.30	Kato et al. (2012a)
V355 UMa	0.057289(1)	0.058183(5)	0.066	0.38	Kato et al. (2012a)
BW Scl	0.0543234(7)	0.055100(2)	0.067	0.37	Kato et al. (2013)

*Orbital period (d).

†Period of late-stage superhumps (d).

‡Estimated disk radius (unit in binary separation).

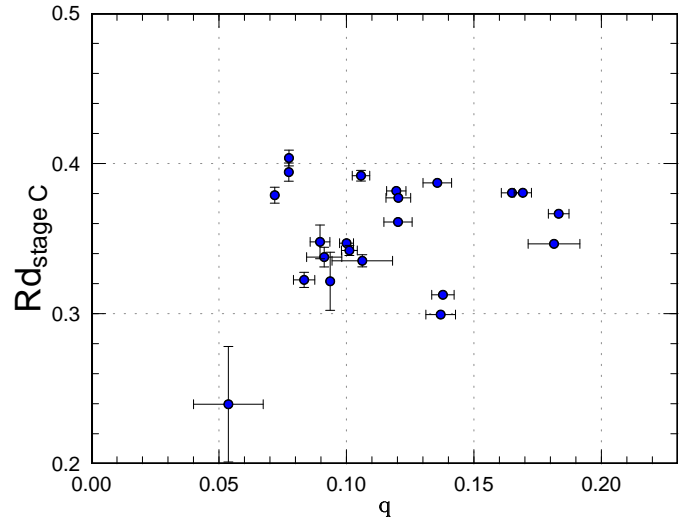
Table 5. Disk radii estimated from the periods of stage C superhumps.

Object	Year	R_{disk}	error
V466 And	2008	0.322	0.005
VY Aqr	2008	0.335	0.004
WX Cet	1989	0.322	0.019
WX Cet	1998	0.338	0.007
V632 Cyg	2008	0.392	0.004
UV Per	2003	0.313	0.002
SW UMa	2006	0.347	0.003
KS UMa	2003	0.382	0.002
HV Vir	2002	0.379	0.005
1RXS J0423	2008	0.380	0.001
ASAS J0233	2006	0.348	0.011
ASAS J1025	2006	0.377	0.002
ASAS J1600	2005	0.299	0.002
SDSS J1556	2007	0.387	0.003
V592 Her	2010	0.240	0.038
IY UMa	2009	0.361	0.002
OT J1044	2010	0.394	0.006
V1504 Cyg	2009b	0.346	0.001
V344 Lyr	2009	0.381	0.001
V344 Lyr	2009b	0.367	0.001
SW UMa	2010	0.404	0.005
OT J210950	2011	0.342	0.003

without measurements of stage A superhumps with an uncertainty of about $\pm 20\%$. An object with a large deviation from the general trend (V592 Her) can be understood as a result of poor observation during the late stage.

4.4. ER UMa Stars and Implication to TTI Model

So far, none of ER UMa stars, a subgroup of SU UMa stars with very frequent outbursts and short supercycles (Kato, Kunjaya 1995; Robertson et al. 1995; Patterson et al. 1995), has been reported to show stage A superhumps in particular for those systems with a low mass ratio q such as ER UMa and V1159 Ori. This can be understood in the framework of the TTI model as follows. In ER UMa stars, the superoutburst is not triggered by a normal outburst as in many SU UMa-type dwarf novae, but the 3:1 resonance starts to appear before the onset of the superoutburst (“Case C” superoutburst in Osaki,

**Fig. 10.** Disk radius estimated from stage C superhumps, assuming that the pressure effect can be neglected.

Meyer 2003, Osaki 2005) because the disk becomes larger than the 3:1 resonance even in quiescence. In this case, the tidal instability triggers the superoutburst. In such a condition, the superhump wave is not restricted to the 3:1 resonance radius at the onset of the superoutburst, and the pressure effect is expected to be already strong, i.e. the object is already in stage B in the early phase of the superoutburst. Although true stage A may be found when the object is still in quiescence, it may be difficult to detect because the luminosity of the disk is much lower than in the superoutburst.

The result that the q values from stage A superhumps very well reproduces the q values from quiescent eclipse observations verifies that our assumption that the disk radius is close to the 3:1 resonance when the superhumps start to emerge. This is the very consequence of the TTI model, and the present result (and the lack of stage A superhumps in ER UMa stars) again strengthens the TTI model.

4.5. Quiescent Superhumps in AL Com and Other Systems

Abbott et al. (1992) detected a very long-period superhump period (89.6 min = 0.0622 d) in AL Com in quiescence. This period has $\varepsilon^*=0.089$, and Patterson et al. (1996) suggested such a large ε^* could arise from the disk close to the 2:1 resonance. We consider this case. Since the q value is not well known in AL Com, we used $q=0.078$ of WZ Sge, which has very similar P_{orb} and P_{SH} to AL Com. Because the pressure effect can be neglected in the quiescent disk, we can use the method in subsection 4.3.1. We could obtain $\varepsilon^*=0.089$ at a disk radius of $0.66A$. This is close to the radius for the 2:1 resonance ($0.61A$ for $q=0.078$). Considering the uncertainty in q , this result seems to support the interpretation by Patterson et al. (1996).

Similar signals, although they may have not been as obvious to be directly seen in the raw light curve as in AL Com, have been reported in other systems: BW Scl ($\varepsilon^*=0.104$, Uthas et al. 2012), possibly EQ Lyn ($\varepsilon^*=0.13$, Szkody et al. 2010) and V455 And [ε^* may be 0.084 if one-day alias is allowed for the data in Araujo-Betancor et al. (2005), (Szkody et al. 2010)]. Using our $q=0.067$ for BW Scl, the large ε^* requires a disk radius of $0.70A$. Even allowing $q=0.073$, it requires $0.69A$. The value for EQ Lyn is even larger, and these (possibly transient) phenomena may be different from superhumps.

5. Summary

We have examined an assumption that the superhump period during the early growing stage of superhumps (stage A superhumps) reflects the dynamical precession rate at the 3:1 resonance, a picture introduced in Osaki, Kato (2013). We have found that the q values estimated from this assumption and q values from quiescent eclipse observations are in good agreement. This led to q estimation of a number of SU UMa-type dwarf novae without measured q values. The obtained q values followed the same CV evolutionary sequence in $P_{\text{orb}} - q$ diagram determined from quiescent eclipse observations in the literature, and we consider this agreement strengthens the validity of our method. Our method gave systematically larger q for short- P_{orb} systems (WZ Sge-type dwarf novae) compared to Patterson (2011), which we interpret as a result of the stronger pressure effect in low- q systems in his case. This difference indicates that the most of the secondaries of known WZ Sge-type dwarf novae are near the border between lower main-sequence and brown dwarfs, and the mass of the secondary at the period minimum is higher than in Patterson (2011). Using our q values, we provide new experimental formulae to convert the observed period excess of fully grown superhumps (stage B superhumps) to q . This method was also used to estimate the disk radius after the termination of superoutburst.

Our study particularly suggests that estimation of ε^* from observations of stage A superhumps can rival the accuracy of the quiescent eclipse observations, and the esti-

ated q from stage A superhumps may be even considered as accurate as q estimates by other dynamical methods. This leads to a very important suggestion to future observations: since stage A lasts only for 1–2 d, it is crucial to start observing superhumps immediately following the onset of the superoutburst, and multi-longitudinal observations are indispensable to record a phase lasting only for 1–2 d. Such a requirement for observation naturally explains why “stage A superhump” only became apparent in this modern era: it is a direct outcome of world-wide cooperation of amateur-professional observers and immediate announcements of outburst detections via internet (no outbursts have been kept secret!), both of which we, especially the VSNET Collaboration (Kato et al. 2004b), have been striving for. Our present research predicts that more coordinated immediate notifications and intensive multi-longitudinal observations in the very early stage of already known and newly discovered SU UMa-type dwarf novae will bring many more q estimations to life whose number can easily surpass the past q estimates of DNe obtained by analyzing quiescent eclipses or radial-velocity studies mobilizing huge telescopes. It will certainly enrich our understanding of the still poorly known late stage of CV evolution. And this is now feasible with distributed small telescope around the globe – why don’t you proceed in this way!

We express our thanks to a discussion with Prof. S. Kato for the relative strength of the pressure and dynamical effects.

References

- Abbott, T. M. C., Robinson, E. L., Hill, G. J., & Haswell, C. A. 1992, *ApJ*, 399, 680
Araujo-Betancor, S., et al. 2005, *A&A*, 430, 629
Augusteyn, T., & Wisotzki, L. 1997, *A&A*, 324, L57
Aungwerojwit, A., et al. 2006, *A&A*, 455, 659
Baptista, R., Catalán, M. S., Horne, K., & Zilli, D. 1998, *MNRAS*, 300, 233
Borges, B. W., & Baptista, R. 2005, *A&A*, 437, 235
Feline, W. J., Dhillon, V. S., Marsh, T. R., & Brinkworth, C. S. 2004, *MNRAS*, 355, 1
Feline, W. J., Dhillon, V. S., Marsh, T. R., Watson, C. A., & Littlefair, S. P. 2005, *MNRAS*, 364, 1158
Gänsicke, B. T., et al. 2009, *MNRAS*, 397, 2170
Gänsicke, B. T., et al. 2006, *MNRAS*, 365, 969
Goodchild, S., & Ogilvie, G. 2006, *MNRAS*, 368, 1123
Harrison, T. E., Hamilton, R. T., Tappert, C., Hoffman, D. I., & Campbell, R. K. 2013, *AJ*, 145, 19
Hellier, C. 2001, *Cataclysmic Variable Stars: How and why they vary* (Berlin: Springer-Verlag)
Hirose, M., & Osaki, Y. 1990, *PASJ*, 42, 135
Hirose, M., & Osaki, Y. 1993, *PASJ*, 45, 595
Horne, K., Wood, J. H., & Stiening, R. F. 1991, *ApJ*, 378, 271
Howell, S. B., Nelson, L. A., & Rappaport, S. 2001, *ApJ*, 550, 897
Imada, A., & Monard, L. A. G. B. 2006, *PASJ*, 58, L19
Ioannou, Z., Naylor, T., Welsh, W. F., Catalán, M. S., Worraker, W. J., & James, N. D. 1999, *MNRAS*, 310, 398
Kato, T., et al. 2013, *PASJ*, 65, 23
Kato, T., et al. 2009, *PASJ*, 61, S395

- Kato, T., & Kunjaya, C. 1995, PASJ, 47, 163
Kato, T., et al. 2012a, PASJ, 64, 21
Kato, T., Maehara, H., & Monard, B. 2008, PASJ, 60, L23
Kato, T., Maehara, H., & Uemura, M. 2012b, PASJ, 64, 62
Kato, T., et al. 2010, PASJ, 62, 1525
Kato, T., Nogami, D., Matsumoto, K., & Baba, H. 2004a, PASJ, 56, S109
Kato, T., & Osaki, Y. 2013, PASJ, in press (arXiv astro-ph/1305.5636)
Kato, T., Uemura, M., Ishioka, R., Nogami, D., Kunjaya, C., Baba, H., & Yamaoka, H. 2004b, PASJ, 56, S1
Knigge, C. 2006, MNRAS, 373, 484
Knigge, C., Baraffe, I., & Patterson, J. 2011, ApJS, 194, 28
Kolb, U. 1993, A&A, 271, 149
Kolb, U., & Baraffe, I. 1999, MNRAS, 309, 1034
Littlefair, S. P., et al. 2013, MNRAS, 431, 2820
Littlefair, S. P., Dhillon, V. S., Marsh, T. R., & Gänsicke, B. T. 2006a, MNRAS, 371, 1435
Littlefair, S. P., Dhillon, V. S., Marsh, T. R., Gänsicke, B. T., Southworth, J., Baraffe, I., Watson, C. A., & Copperwheat, C. 2008, MNRAS, 388, 1582
Littlefair, S. P., Dhillon, V. S., Marsh, T. R., Gänsicke, B. T., Southworth, J., & Watson, C. A. 2006b, Science, 314, 1578
Lubow, S. H. 1992, ApJ, 401, 317
Mineshige, S., Hirose, M., & Osaki, Y. 1992, PASJ, 44, L15
Montgomery, M. M. 2001, MNRAS, 325, 761
Murray, J. R. 1998, MNRAS, 297, 323
Osaki, Y. 1985, A&A, 144, 369
Osaki, Y. 1989, PASJ, 41, 1005
Osaki, Y. 1995, PASJ, 47, 47
Osaki, Y. 1996, PASP, 108, 39
Osaki, Y. 2005, Proc. Japan Acad. Ser. B, 81, 291
Osaki, Y., & Kato, T. 2013, PASJ, in press (arXiv astro-ph/1305.5877)
Osaki, Y., & Meyer, F. 2003, A&A, 401, 325
Patterson, J. 1998, PASP, 110, 1132
Patterson, J. 2011, MNRAS, 411, 2695
Patterson, J., Augusteijn, T., Harvey, D. A., Skillman, D. R., Abbott, T. M. C., & Thorstensen, J. 1996, PASP, 108, 748
Patterson, J., Jablonski, F., Koen, C., O'Donoghue, D., & Skillman, D. R. 1995, PASP, 107, 1183
Patterson, J., et al. 2005, PASP, 117, 1204
Patterson, J., et al. 1998, PASP, 110, 1290
Patterson, J., et al. 2002, PASP, 114, 721
Patterson, J., et al. 2003, PASP, 115, 1308
Patterson, J., et al. 2000, PASP, 112, 1584
Pearson, K. J. 2006, MNRAS, 371, 235
Robertson, J. W., Honeycutt, R. K., & Turner, G. W. 1995, PASP, 107, 443
Savoury, C. D. J., et al. 2011, MNRAS, 415, 2025
Shears, J. H., Gänsicke, B. T., Brady, S., Dubovsky, P., Miller, I., & Staels, B. 2011, New Astron., 16, 311
Sheets, H. A., Thorstensen, J. R., Peters, C. J., Kapusta, A. B., & Taylor, C. J. 2007, PASP, 119, 494
Smak, J. 2009, Acta Astron., 59, 121
Southworth, J., & Copperwheat, C. M. 2011, Observatory, 131, 66
Southworth, J., Copperwheat, C. M., Gänsicke, B. T., & Pyzas, S. 2010, A&A, 510, A100
Steehgs, D., Howell, S. B., Knigge, C., Gänsicke, B. T., Sion, E. M., & Welsh, W. F. 2007, ApJ, 667, 442
Steehgs, D., Marsh, T., Knigge, C., Maxted, P. F. L., Kuulkers, E., & Skidmore, W. 2001, ApJL, 562, L145
Steehgs, D., Perryman, M. A. C., Reynolds, A., de Bruijne, J. H. J., Marsh, T., Dhillon, V. S., & Peacock, A. 2003, MNRAS, 339, 810
Sterken, C., Vogt, N., Schreiber, M. R., Uemura, M., & Tuvikene, T. 2007, A&A, 463, 1053
Szkody, P., et al. 2010, ApJ, 710, 64
Thorstensen, J. R. 2003, AJ, 126, 3017
Thorstensen, J. R., & Fenton, W. H. 2003, PASP, 115, 37
Thorstensen, J. R., Patterson, J. O., Kemp, J., & Vennes, S. 2002, PASP, 114, 1108
Thorstensen, J. R., & Taylor, C. J. 1997, PASP, 109, 1359
Uemura, M., Kato, T., Nogami, D., & Ohsugi, T. 2010, PASJ, 62, 613
Uthas, H., et al. 2012, MNRAS, 420, 379
Wade, R. A., & Horne, K. 1988, ApJ, 324, 411
Warner, B. 1995, Cataclysmic Variable Stars (Cambridge: Cambridge University Press)
Whitehurst, R. 1988, MNRAS, 232, 35
Woudt, P. A., Warner, B., de Budé, D., Macfarlane, S., Schurch, M. P. E., & Zietsman, E. 2012, MNRAS, 421, 2414
Woudt, P. A., Warner, B., & Pretorius, M. L. 2004, MNRAS, 351, 1015